

Published in final edited form as:

*Invest Ophthalmol Vis Sci.* 2009 April ; 50(4): 1552–1558. doi:10.1167/iovs.08-2455.

## Evaluation of the X-Linked High-Grade Myopia Locus (MYP1) with Cone Dysfunction and Color Vision Deficiencies

Ravikanth Metlapally<sup>1,2</sup>, Michel Michaelides<sup>3,4</sup>, Anuradha Bulusu<sup>2</sup>, Yi-Ju Li<sup>2</sup>, Marianne Schwartz<sup>5</sup>, Thomas Rosenberg<sup>6</sup>, David M. Hunt<sup>3</sup>, Anthony T. Moore<sup>3,4</sup>, Stephan Züchner<sup>2</sup>, Catherine Bowes Rickman<sup>1</sup>, and Terri L. Young<sup>1,2</sup>

<sup>1</sup>Duke University Eye Center, Durham, North Carolina

<sup>2</sup>Duke University Center for Human Genetics, Durham, North Carolina

<sup>3</sup>Institute of Ophthalmology, University College London, London, United Kingdom

<sup>4</sup>Moorfields Eye Hospital, London, United Kingdom

<sup>5</sup>National Eye Clinic for the Visually Impaired, Copenhagen, Denmark

<sup>6</sup>Gordon Norrie Centre, National Eye Clinic, Hellerup, Denmark

### Abstract

**Purpose**—X-linked high myopia with mild cone dysfunction and color vision defects has been mapped to chromosome Xq28 (MYP1 locus). *CXorf2/TEX28* is a nested, intercalated gene within the red-green opsin cone pigment gene tandem array on Xq28. The authors investigated whether TEX28 gene alterations were associated with the Xq28-linked myopia phenotype. Genomic DNA from five pedigrees (with high myopia and either protanopia or deuteranopia) that mapped to Xq28 were screened for TEX28 copy number variations (CNVs) and sequence variants.

**Methods**—To examine for CNVs, ultra-high resolution array-comparative genomic hybridization (array-CGH) assays were performed comparing the subject genomic DNA with control samples (two pairs from two pedigrees). Opsin or TEX28 gene-targeted quantitative real-time gene expression assays (comparative CT method) were performed to validate the array-CGH findings. All exons of TEX28, including intron/exon boundaries, were amplified and sequenced using standard techniques.

**Results**—Array-CGH findings revealed predicted duplications in affected patient samples. Although only three copies of TEX28 were previously reported within the opsin array, quantitative real-time analysis of the TEX28 targeted assay of affected male or carrier female individuals in these pedigrees revealed either fewer (one) or more (four or five) copies than did related and control unaffected individuals. Sequence analysis of TEX28 did not reveal any variants associated with the disease status.

**Conclusions**—CNVs have been proposed to play a role in disease inheritance and susceptibility as they affect gene dosage. TEX28 gene CNVs appear to be associated with the MYP1 X-linked myopia phenotypes.

---

Copyright © Association for Research in Vision and Ophthalmology

Corresponding author: Terri L. Young, Duke University Center for Human Genetics, 595 La Salle Street, Durham, NC 27710; tyoung@chg.duhs.duke.edu.

Disclosure: **R. Metlapally**, None; **M. Michaelides**, None; **A. Bulusu**, None; **Y.-J. Li**, None; **M. Schwartz**, None; **T. Rosenberg**, None; **D.M. Hunt**, None; **A.T. Moore**, None; **S. Züchner**, None; **C. Bowes Rickman**, None; **T.L. Young**, None

Numerous genetic linkage studies have identified chromosomal regions associated with primarily familial development of myopia.<sup>1</sup> In the present study, we evaluated pedigrees that mapped to the first identified locus for high myopia on chromosome X (MYP1, OMIM 310460).<sup>2</sup> In a large pedigree reported in 1988, this locus was mapped to chromosome Xq27.3–28 by Schwartz et al.<sup>2–4</sup> and Young et al.<sup>2–4</sup> using restriction fragment-linked polymorphic markers. The family originated in Bornholm, Denmark, and the phenotype of Bornholm eye disease (BED) included high-grade myopia, amblyopia, optic nerve hypoplasia, subnormal dark-adapted electroretinographic (ERG) flicker function, and deuteranopia. In 2004, Young et al.<sup>4</sup> reported another high-grade myopia phenotype in a family of Danish descent living in Minnesota that mapped to the Xq28 locus, with a similar phenotype of optic nerve hypoplasia with temporal pigmentary crescent, subnormal photopic ERG function, and protanopia rather than deuteranopia in the BED phenotype. We suggested that the phenotype was more consistent with an X-linked cone dysfunction than with simplex myopia. A recent replication report from the United Kingdom confirmed the X-linked cone dysfunction syndrome with an associated moderate to high myopia and protanopia phenotype.<sup>5</sup>

Although the X-linked myopia phenotypes are similar, a distinguishing feature is the type of color vision deficiency, which is deuteranopia in the BED pedigree and protanopia in the Minnesota and United Kingdom pedigrees. Interestingly, the visual cone pigment (opsin) genes, red (long wavelength [L]) and green (medium wavelength [M]), are present in tandem on the human X-chromosome at Xq28. In this opsin gene array, a single L, or red, gene is followed by one or more copies of the M, or green, gene in the normal color vision state.<sup>6,7</sup> Alterations in this gene array with a red-green opsin hybrid gene in the first position or a green-red opsin hybrid in the second position are associated with protan and deutan color vision defects, respectively.<sup>7,8</sup> Young et al.<sup>4</sup> performed single-stranded conformational polymorphism analysis to determine the ratio of red to green promoters in the BED and Minnesota pedigrees. We previously determined that affected and unaffected males in both pedigrees had four and three opsin genes, respectively, and reported that known reported hybrid opsin genes are responsible for the respective color vision deficiencies.<sup>4</sup>

The opsin gene array represents a region of repetitive DNA segments termed *segmental duplications*. The segmental duplications involving opsin genes encompass the testis-expressed protein 28 gene (TEX28), also known as chromosome X open-reading frame 2 (CXorf2), a nested gene within the cone opsin pigment gene array.<sup>9</sup> TEX28 is composed of five exons that almost span the entire distance between the protein-coding regions of the opsin genes and the transketolase-related type 1 gene (*TKTL1*), and it encodes a polypeptide of 410 amino acid residues (Fig. 1). Few studies of TEX28 have been reported in the literature, and its involvement in the X-linked myopia phenotypes is unknown.<sup>10,11</sup> The reported number of normal repetitive copies of TEX28 is three, intercalated within and translated in the opposite (3' to 5') direction from the opsin gene array.<sup>9</sup>

Because of the consistent color vision deficiencies in all reported MYP1 pedigrees, we hypothesized that the X-linked MYP1 myopia phenotype could be caused by TEX28 sequence alterations or copy number variation (CNV). This was determined using fine mapping array comparative genomic hybridization (array-CGH) and real-time quantitative polymerase chain reaction (RT-qPCR) assays. Sequence mutation screening, genetic association, and gene expression studies were also performed.

## Materials and Methods

### Subjects

Informed consent was obtained from all participants, and venous blood and clinical ophthalmologic data were obtained from all study participants. Total genomic DNA was extracted from venous blood with the use of reagents (AutoPure LS DNA Extractor and PUREGENE; Genra Systems, Minneapolis, MN). The study was approved by the institutional review boards at the Duke University Medical Center, National Eye Clinic for the Visually Impaired at Hellerup, and the Mooresfield Eye Hospital, and it followed the principles of the Declaration of Helsinki. Selected member DNA samples from the BED,<sup>2</sup> Minnesota,<sup>4</sup> and United Kingdom pedigrees<sup>5</sup> were used in this study.

### Copy Number Variation Screening Using Array-CGH

DNA copy number differences of genetic intervals on chromosome X between affected and unaffected member DNA samples from the BED and the Minnesota pedigrees were determined using a high-definition, finetiling, array-CGH platform (NimbleGen Systems, Madison, WI) according to the manufacturer's instructions. Briefly, reference (unaffected male from within the pedigree) and test (affected male from within the pedigree) DNA samples were differentially labeled with fluorescent tags (Cy5 and Cy3, respectively) and were hybridized to genomic arrays after repetitive element binding was blocked with the use of COT-1 DNA. After hybridization, the fluorescence ratio (Cy3/Cy5) was calculated to reveal the copy number differences between the two DNA samples. Four mi-croarray chips were used to screen two sets from each pedigree (one set contained an affected and an unaffected DNA sample). The average single nucleotide polymorphism probe spacing for the X chromosome array-CGH chip measured 340 base pairs (bp).

### Copy Number Variation Screening Using Real-Time PCR

To validate the results obtained from the array-CGH method, real-time PCR gene expression assays (Assays-by-Design; Applied Biosystems, Foster City, CA) consisting of a mix of unlabeled PCR primers and the minor groove-binding group (MGB) probe (FAM and VIC dye-labeled TaqMan; Applied Biosystems) were designed for the opsin genes and TEX28 sequences to quantitate expression of these genes at the genomic DNA level. The assay targeted opsin genes (not distinguishing between the red and green opsin variants) to validate the sensitivity of the experiment as the number of opsin copies were known for the BED and Minnesota pedigrees.<sup>4</sup> The assay on TEX28 was performed on 14 family members from the BED and Minnesota pedigrees (seven from each pedigree: three affected males, two unaffected males, and two carrier females). Patient DNA samples from the United Kingdom pedigrees were screened as well, but family sample sizes were variable and comparatively limited. Family 1 contained one affected male, one unaffected male, and one carrier female. Family 2 contained two affected males, one unaffected male, and one carrier female. Family 3 contained one affected male and one unaffected male. An assay for the ubiquitous housekeeping gene *GAPDH* served as an endogenous reference. All assays were tested across a broad template dilution range, and amplification efficiency was equivalent across all assays. All reactions were matched for the starting sample amount and were run in quadruplicate.

Real-time PCR reactions were performed (TaqMan Universal PCR Master Mix with the ABI7900HT Fast Real-time PCR System; Applied Biosystems). Data were analyzed using the comparative  $C_T$  method, by which the amount of target normalized to an endogenous reference and relative to a calibrator (known individual value) is calculated as  $2^{-(\delta\delta C_T)}$  (user bulletin 2; ABI Sequence Detection Systems; Applied Biosystems;  $\delta\delta C_T$  is the difference between the normalized cycle threshold of an unknown sample and the normalized cycle

threshold of the calibrator). Results were plotted as the number of copies present in each individual with respect to the assigned number of copies in the calibrator.

### **Polymerase Chain Reactions, Sequencing, and Genetic Analyses**

Primer pairs were designed to amplify the identified five exons of TEX28 incorporating the 5' and 3' UTRs, covering 50 to 150 bp of each intron-exon boundary. PCR amplifications were performed on subject genomic DNA (Platinum *Taq* DNA polymerase; Invitrogen, Carlsbad, CA) with the use of a touchdown protocol (available on request). Amplicons were visualized using agarose gel electrophoresis and were purified (Quickstep 2 SOPE Resin; Edge BioSystems, Gaithersburg, MD). Sequencing reactions were performed (BigDye Terminator on the ABI3730 or 3100 Genetic Analyzer; Applied Biosystems). Sequences were trimmed for quality and were aligned with a software program (Sequencher; Gene Codes, Ann Arbor, MI). Individual DNA sequences were compared alongside the known reference sequence for TEX28 (UCSC Genome Browser [<http://genome.ucsc.edu/>] Representative Refseq: NM001586).

### **TEX28 Gene Expression**

An RNA panel (Human Total RNA Master Panel II; Clontech Laboratories, Palo Alto, CA) was used to investigate the expression pattern of TEX28 in various human organ tissue types. The panel consisted of RNA from 21 tissue types. Healthy human donor eyes were obtained from the North Carolina Eye Bank (<http://www.nceyebank.org/>), an organization dedicated to providing eye tissue for transplantation and research efforts. Enucleated eyes were stored (RNAlater; Ambion, Austin, TX) within 4 to 6 hours of death. Retina, retinal pigment epithelium (RPE)-choroid complex, and sclera were separated by fine dissection from 6-mm trephine punches taken from the posterior pole, where most scleral distension/retinal thinning occurs in myopia. Total RNA from each tissue layer was isolated (Ribopure kit; Applied Biosystems/Ambion). RNA was converted to cDNA by a commercial reverse transcription system (Promega, Madison, WI). PCR amplifications were performed with TEX28-specific primers, and amplicons were visualized by agarose gel electrophoresis. GAPDH-specific primers were used as positive controls across all tissue types. GAPDH primers also helped rule out genomic contamination (two distinct amplicons were expected if genomic contamination was present).

### **Genotyping**

A custom allelic discrimination assay (TaqMan; Applied Biosystems) consisting of a mix of unlabeled polymerase chain reaction (PCR) primers and the MGB probe (FAM and VIC dye-labeled TaqMan; Applied Biosystems) was used to genotype the novel 5'UTR SNP of TEX28 in a larger case-control cohort that included subject DNA from affected and unaffected males (total, 195). This assay consisted of two unlabeled PCR primers and two allele-specific probes. PCR reactions were performed (TaqMan Universal PCR Master Mix on the GeneAmp PCR System 9700; Applied Biosystems), and a PCR system (ABI7900HT Fast PCR System; Applied Biosystems) was used to read the allelic discrimination calls.

### **Statistical Analyses**

For genotyping data, the Fisher exact test was performed to determine the incidence of the 5' UTR SNP in subject DNA from unaffected males and was compared with that in the affected males ( $-5 D$ ). For array-CGH microarray data, the DNA segmentation analysis of averaged  $\log_2$  ratios was performed using the circular binary segmentation algorithm<sup>12</sup> implemented in software (NimbleScan; NimbleGen Systems). All calls were made when  $P < 0.01$ .

## Results

### Copy Number Variation Screening of the Xq28 Region Using Array-CGH

Array-CGH results revealed copy number variations in the affected samples in the region of the opsin gene array in the BED and the Minnesota pedigrees (Fig. 2). Both pedigrees showed predicted duplications in this region. The  $\log_2$  ratio, which was calculated by subtracting the log value of the reference sample intensity from the log of the test sample intensity, was greater than +0.25 in this region (0.1-0.25, potential single copy change; 0.25-0.8, single copy change; >0.8, 2-copy change). Figure 3 illustrates a close-up view of the predicted duplication in the opsin gene region in the BED phenotype. In addition, the array with the Minnesota pedigree sample revealed an approximately 28-kb intergenic deletion (predicted location, 154046000-154074000 bp) in the subject DNA samples of affected males between a BRCA1-BRCA2-containing complex 3 (*BRCC3*), which is an E3 ubiquitin ligase, and von Hippel-Lindau binding protein 1 (*VBPI*; Fig. 2). The Minnesota pedigree subject DNA of affected males also had an approximately 8-kb intergenic duplication between sprouty homolog 3 (*SPRY3*) and trimethyl lysine hydroxylase, epsilon (*TMLHE*; Fig. 2).

To emphasize the quality of array-CGH data, scatter plots for each of the four arrays with  $\log_2(\text{Cy3 intensity})$  and  $\log_2(\text{Cy5 intensity})$  on the *x*- and *y*-axes, respectively, are provided in Supplementary Figure S1, <http://www.iovs.org/cgi/content/full/50/4/1552/DC1>. These calculations were made without normalization and background correction. Regression statistics ( $R^2 > 0.92$ ;  $P < 10^{-10}$ ) indicated a good overall linear relationship between Cy3 and Cy5 intensities in the Xq28 region. Copy number differences were calculated based on significant differences in these signal intensities.

### Copy Number Variation Screening Using Real-Time PCR

The assay targeted on the opsin genes (Fig. 4a) confirmed the expected number of copies of the opsin genes<sup>4</sup> present in subject DNA of affected males (four copies), related and control males (three copies), and a carrier female (seven copies) in the Minnesota pedigree. Results with the assay targeted on the *TEX28* gene indicated that affected males in the Minnesota pedigree had up to five copies of *TEX28* (Fig. 4b), unaffected males had three copies, and carrier females had eight copies. Similarly, the subject DNA of affected males in the BED pedigree revealed four copies and that of unaffected males revealed three copies (Fig. 4c). Subject DNA of pedigrees from the United Kingdom with protanopia showed fewer or greater numbers of copies in affected individuals than in unaffected individuals (Fig. 5). For the pedigrees from the United Kingdom, it was assumed that unaffected persons had three copies of *TEX28*. In Family 1, affected male DNA sample showed four copies. In Family 2, no difference was seen between affected and unaffected persons, and the DNA sample of an affected male from Family 3 revealed one copy of the gene.

### Polymerase Chain Reactions, Sequencing, Genotyping, and Genetic Analyses

Mutation screening of *TEX28* revealed a novel SNP in the 5' UTR (nucleotide position -8' upstream of the initiation codon) that segregated with the affection status in the Minnesota pedigree and the United Kingdom Family 2 pedigree, both of the X-linked myopia phenotype with protanopia. This was revealed in DNA samples of all four affected males and two carrier females screened, whereas the unaffected males (three) and controls married into the pedigree (two) did not show this polymorphism. This SNP was screened in a larger dataset (195 males) by means of an allelic discrimination assay (TaqMan; Applied Biosystems) and Fisher exact test to compare the incidence of this SNP in DNA samples of unaffected males and affected males ( $-5 D$ ) and revealed no significant difference ( $P = 0.6$ ).

Primer pairs (two within the deletion and two flanking) were designed to confirm the 28-kb deletion between *BRCC3* and *VBPI* using PCR in the Minnesota family. As expected, samples from the affected patient did not reveal amplicons in the deleted region, but amplicons were observed flanking the predicted deletion (Fig. 6), and the unaffected patient sample DNA showed amplification with all primer sets. PCR was performed with primer pairs within the deletion in the United Kingdom pedigree samples, and no deletion was detected (data not shown).

### Profiling of TEX28 Gene Expression

Expression of TEX28 was examined by RT-PCR using a panel containing 21 normal human organ tissue types. TEX28 was expressed in three of the tissue types tested— blood, kidney, and testis (Fig. 7). In the ocular tissues examined, the retina, sclera, cornea, optic nerve, and trabecular meshwork showed TEX28 expression (Fig. 8). The non-template controls (negative controls using sterile water) did not show expression. GAPDH primers amplified the region of interest in all cDNA samples and served as positive controls.

### Discussion

The X-linked high-grade myopia phenotypes investigated in this study are complex, with characteristics that include features such as amblyopia, optic nerve hypoplasia, cone photoreceptor dysfunction, and red-green or green-red color vision deficiencies. In this work, we evaluated and addressed an aspect of X-linked high-grade myopia at the genomic level by performing screening studies on a potential candidate gene.

Segmental duplications have been implicated in disorders that result from inappropriate gene dosage.<sup>13,14</sup> Segmental duplications can mediate cytogenetic alterations such as deletions, duplications, translocations, and inversions, which can give rise to an altered number of copies at the genomic level leading to altered dosage.<sup>15</sup> Examples of genetic disorders mediated by altered gene dosage include Charcot-Marie-Tooth disease type 1A (CMT1A),<sup>16,17</sup> Smith-Magenis syndrome,<sup>18</sup> neurofibromatosis type 1,<sup>19</sup> X-linked ichthyosis,<sup>20</sup> and hemophilia A.<sup>21</sup> Complex disorders such as Parkinson disease,<sup>22</sup> early-onset Alzheimer disease,<sup>23</sup> and hereditary pancreatitis<sup>24</sup> have also been associated with CNV.

In recent times, CNV has been speculatively involved in susceptibility to and etiology of various conditions, including complex multifactorial traits.<sup>25,26</sup> The results obtained in our study are in agreement with this line of thought. The array-CGH data revealed CNVs in DNA samples of affected male subjects of the BED and Minnesota pedigrees in the Xq28 region involving the opsin gene array. Both pedigrees showed predicted duplications in this region, which includes opsin cone pigment and TEX28 genes. CNVs in this region can occur because of the close homology of the genes, making them susceptible to unequal crossing over during meiosis. The realtime assay targeted on the opsin genes confirmed previous predicted findings of opsin gene numbers in the Minnesota pedigree.<sup>4</sup> Only three copies of TEX28 have been reported within the opsin gene array,<sup>9,11</sup> though the real-time assay targeted on the TEX28 gene indicated that the affected male subjects had up to four copies of TEX28 in the BED and five copies in the Minnesota phenotypes in contrast to the 3 copies in the unaffected males. Two families from the United Kingdom showed either fewer (one) or greater (four) number of copies in the affected samples when compared with the unaffected samples.

Triplication of the  $\alpha$ -synuclein locus (OMIM 163890) is causal for Parkinson disease,<sup>22</sup> and duplication of the amyloid beta A4 precursor protein locus (OMIM 104760) has been reported to cause early-onset Alzheimer disease and cerebral amyloid angiopathy,<sup>23</sup> all of

which are considered complex diseases. Similarly, in CMT1A (OMIM 601097), duplication involving the peripheral myelin protein 22 (*PMP22*) gene on chromosome 17p12 has been reported, and it is speculated that the decreased nerve conduction velocities observed are a consequence of gene dosage effect.<sup>17</sup> We speculate that the CNVs we observed in the opsin gene array region may play a role in the X-linked high-grade myopia phenotypes evaluated. The relative higher/lower number of opsin genes in affected male subject DNA may not play a role in color vision deficiencies because the red-green and green-red hybrid genes reported previously<sup>4</sup> explain the color vision associations in the tested Minnesota and BED pedigrees. Moreover, it is known that only the first two opsin genes are expressed in the retina.<sup>27</sup> The relative change in the number of *TEX28* copies could be involved in phenotypes with opsin gene arrays containing red-green/green-red hybrid genes such as the ones investigated in this study. No substantive evidence demonstrates which *TEX28* copies are functional because the entire protein coding sequence of *TEX28* exists in all the copies. Hence, the exact manner by which *TEX28* gene regulation might play a role is unknown and requires further investigation. It is also likely that the *TEX28* CNVs observed are an indication of a true causal variation in linkage disequilibrium (LD) with these CNVs. The fewer copies observed in United Kingdom Family 2 and Family 3 prompted us to ask whether their phenotypes were different from those in BED, Minnesota, and United Kingdom Family 1. All five families investigated had myopia, cone photoreceptor dysfunction, and red-green or green-red color vision deficiencies as clinical features. To the best of our knowledge, United Kingdom Family 2 and Family 3 do not have any unique features. It is possible that *TEX28* variations may not explain all the phenotypes of X-linked myopia examined. The inconsistent genotype-phenotype correlation observed in Family 2 and Family 3 may also suggest the involvement of a variant in LD with *TEX28* CNVs.

There were differences in the *TEX28* copy gain or loss among the Minnesota, BED, and United Kingdom pedigrees. If one assumes that *TEX28* is a nested gene and always follows an opsin gene within the array, the findings in the subject DNA of affected males in the Minnesota pedigree point otherwise (five *TEX28* copies, four opsins), indicating an extra copy gain of *TEX28* in relation to the opsin copy gain. Similarly, the affected males in the United Kingdom pedigrees also showed an unequal loss/gain in *TEX28* copies. It was not possible to determine the precise location of this extra gain/loss of *TEX28* because of the high sequence similarity.

Additionally, the subject DNA of affected males in the Minnesota pedigree showed an intergenic deletion and duplication downstream from the opsin gene array in the Xq28 region. The deletion was confirmed by a nested PCR approach in the affected males in the Minnesota pedigree. The deletion, however, was not further characterized at its borders because it was exclusive to one family and, hence, may not be a common element that explains the high-grade myopia in these pedigrees. Intergenic deletions are associated with disease and have been proposed to play a role in the regulation of transcription of nearby genes by *cis* regulatory action or position effect.<sup>28</sup> However, the potential regulatory effect of this deletion on flanking genes BRCA1-BRCA2-containing complex 3 (BRCC3; 42 kb upstream) and von Hippel-Lindau binding protein 1 (VBP1; 22 kb downstream) requires further investigation. The role of intergenic duplications is unknown, though it is recognized that segmental duplications cause genomic instability.<sup>15</sup> These intergenic alterations were not observed in affected (or unaffected) DNA samples of the BED and the United Kingdom phenotypes (array-CGH and PCR data, respectively).

In addition to CNV, we examined whether *TEX28* showed any sequence variants. Mutation screening revealed a novel SNP in the 5' UTR (nucleotide position 8' upstream of the initiation codon) of the *TEX28* gene that segregated with the affection status in the Minnesota pedigree and one United Kingdom pedigree. However, follow-up study of this

SNP in a larger dataset using an allelic discrimination assay (TaqMan; Invitrogen) revealed no significant association ( $P = 0.6$ ) between the frequencies of the SNP in affected versus unaffected males, thus ruling out any role for this SNP. Several candidate genes on the Xq28 locus were also sequence screened in parallel based on their function and expression profiles and cytogenic location, and no sequence variants were associated with the disease status. The genes that were screened include *CTAG1*, *CTAG2*, *MPP1*, *CLIC2*, *H2AFB3*, *TMLHE*, *SPRY3*, *SYBL1*, *NT\_025307.28*, *NT\_025307.29*, *AFF2*, *CXORF1*, *FMRI*, *IDS*, *MECP2*, *MTM1*, *RENBP*, *GABRA3*, *GDII*, *MAGEA10*, *NSDHL*, *SLITRK2*, *SLITRK4*, *TKTL1*, and *ZNF275*.

Few studies on *TEX28* have been published,<sup>9–11</sup> and the expression studies we performed revealed that *TEX28* is expressed in blood, kidney, and testis at the mRNA level. Although the expression in testis is consistent with previous findings, Chen et al.<sup>29</sup> did not report expression in kidney and did not test for expression in blood. Ocular gene expression experiments conducted in the present study revealed the presence of *TEX28* in five ocular tissues, including the retina and the sclera. Interestingly, in a recent study based on ocular-expression profiles using serial analysis of gene expression, *TEX28* was reported to be expressed in the human retina.<sup>30</sup> Involvement of the retina through a putative retinoscleral signaling cascade has been proposed to play a role in ocular elongation and myopia development.<sup>31</sup> Consequently, the potential regulatory effects of *TEX28* CNV in these layers could be involved in the phenotypes studied.

In summary, our study suggests that array-CGH and realtime PCR are reliable techniques to investigate and validate CNVs. The X-linked high-grade myopia phenotypes with color vision deficiencies studied are associated with *TEX28* CNVs. The role of CNVs in genetic disease is a novel area of research and may explain some forms of X-linked myopia.

## Supplementary Material

Refer to Web version on PubMed Central for supplementary material.

## Acknowledgments

The authors thank all the subjects who participated in this study.

Supported by National Institutes of Health Grant EY014685 and Research to Prevent Blindness Inc.

## References

1. Young TL, Metlapally R, Shay AE. Complex trait genetics of refractive error. *Arch Ophthalmol*. 2007; 125:38–48. [PubMed: 17210850]
2. Schwartz M, Haim M, Skarsholm D. X-linked myopia: Bornholm eye disease. Linkage to DNA markers on the distal part of Xq. *Clin Genet*. 1990; 38:281–286.
3. Haim M, Fledelius HC, Skarsholm D. X-linked myopia in Danish family. *Acta Ophthalmol (Copenh)*. 1988; 66:450–456. [PubMed: 3264103]
4. Young TL, Deeb SS, Ronan SM, et al. X-linked high myopia associated with cone dysfunction. *Arch Ophthalmol*. 2004; 122:897–908.
5. Michaelides M, Johnson S, Bradshaw K, et al. X-linked cone dysfunction syndrome with myopia and protanopia. *Ophthalmology*. 2005; 112:1448–1454.
6. Nathans J, Thomas D, Hogness DS. Molecular genetics of human color vision: the genes encoding blue, green, and red pigments. *Science*. 1986; 232:193–202.
7. Nathans J, Piantanida TP, Eddy RL, Shows TB, Hogness DS. Molecular genetics of inherited variation in human color vision. *Science*. 1986; 232:203–210. [PubMed: 3485310]



8. Deeb SS, Lindsey DT, Hibiya Y, et al. Genotype-phenotype relationships in human red/green color-vision defects: molecular and psychophysical studies. *Am J Hum Genet.* 1992; 51:687–700.
9. Hanna MC, Platts JT, Kirkness EF. Identification of a gene within the tandem array of red and green color pigment genes. *Genomics.* 1997; 43:384–386.
10. Oda S, Ueyama H, Nishida Y, Tanabe S, Yamade S. Analysis of L-cone/M-cone visual pigment gene arrays in females by long-range PCR. *Vision Res.* 2003; 43:489–495. [PubMed: 12594995]
11. Ueyama H, Torii R, Tanabe S, Oda S, Yamade S. An insertion/deletion TEX28 polymorphism and its application to analysis of red/green visual pigment gene arrays. *J Hum Genet.* 2004; 49:548–557.
12. Olshen AB, Venkatraman ES, Lucito R, Wigler M. Circular binary segmentation for the analysis of array-based DNA copy number data. *Biostatistics.* 2004; 5:557–572.
13. Ji Y, Eichler EE, Schwartz S, Nicholls RD. Structure of chromosomal duplicons and their role in mediating human genomic disorders. *Genome Res.* 2000; 10:597–610.
14. Mazzarella R, Schlessinger D. Pathological consequences of sequence duplications in the human genome. *Genome Res.* 1998; 8:1007–1021. [PubMed: 9799789]
15. Emanuel BS, Shaikh TH. Segmental duplications: an ‘expanding’ role in genomic instability and disease. *Nat Rev Genet.* 2001; 2:791–800. [PubMed: 11584295]
16. Chance PF, Abbas N, Lensch MW, et al. Two autosomal dominant neuropathies result from reciprocal DNA duplication/deletion of a region on chromosome 17. *Hum Mol Genet.* 1994; 3:223–228. [PubMed: 8004087]
17. Lupski JR, Wise CA, Kuwano A, et al. Gene dosage is a mechanism for Charcot-Marie-Tooth disease type-1A. *Nat Genet.* 1992; 1:29–33.
18. Chen KS, Manian P, Koeuth T, et al. Homologous recombination of a flanking repeat gene cluster is a mechanism for a common contiguous gene deletion syndrome. *Nat Genet.* 1997; 17:154–163.
19. Dorschner MO, Sybert VP, Weaver M, Pletcher BA, Stephens K. NF1 microdeletion breakpoints are clustered at flanking repetitive sequences. *Hum Mol Genet.* 2000; 9:35–46.
20. Ballabio A, Andria G. Deletions and translocations involving the distal short arm of the human X chromosome: review and hypotheses. *Hum Mol Genet.* 1992; 1:221–227.
21. Naylor JA, Buck D, Green P, Williamson H, Bentley D, Giannelli F. Investigation of the factor VIII intron 22 repeated region (int22h) and the associated inversion junctions. *Hum Mol Genet.* 1995; 4:1217–1224.
22. Singleton AB, Farrer M, Johnson J, et al. alpha-Synuclein locus triplication causes Parkinson's disease. *Science.* 2003; 302:841. [PubMed: 14593171]
23. Rovelet-Lecruz A, Hannequin D, Raux G, et al. APP locus duplication causes autosomal dominant early-onset Alzheimer disease with cerebral amyloid angiopathy. *Nat Genet.* 2006; 38:24–26. [PubMed: 16369530]
24. Le Marechal C, Masson E, Chen JM, et al. Hereditary pancreatitis caused by triplication of the trypsinogen locus. *Nat Genet.* 2006; 38:1372–1374.
25. Beckmann JS, Estivill X, Antonarakis SE. Copy number variants and genetic traits: closer to the resolution of phenotypic to genotypic variability. *Nat Rev Genet.* 2007; 8:639–646.
26. Lupski JR, Stankiewicz P. Genomic disorders: molecular mechanisms for rearrangements and conveyed phenotypes. *PLoS Genet.* 2005; 1:627–633.
27. Hayashi T, Motulsky AG, Deeb SS. Position of a ‘green-red’ hybrid gene in the visual pigment array determines colour-vision phenotype. *Nat Genet.* 1999; 22:90–93. [PubMed: 10319869]
28. Balemans W, Patel N, Ebeling M, et al. Identification of a 52 kb deletion downstream of the SOST gene in patients with van Buchem disease. *J Med Genet.* 2002; 39:91–97. [PubMed: 11836356]
29. Chen YT, Iseli C, Venditti CA, Old LJ, Simpson AJG, Jongeneel CV. Identification of a new cancer/testis gene family, CT47, among expressed multicopy genes on the human X chromosome. *Genes Chromosomes Cancer.* 2006; 45:392–400.
30. Bowes Rickman C, Ebright JN, Zavodni ZJ, et al. Defining the human macula transcriptome and candidate retinal disease genes using EyeSAGE. *Invest Ophthalmol Vis Sci.* 2006; 47:2305–2316. [PubMed: 16723438]

31. Christensen AM, Wallman J. Evidence that increased scleral growth underlies visual deprivation myopia in chicks. *Invest Ophthalmol Vis Sci.* 1991; 32:2143–2150. [PubMed: 2055705]

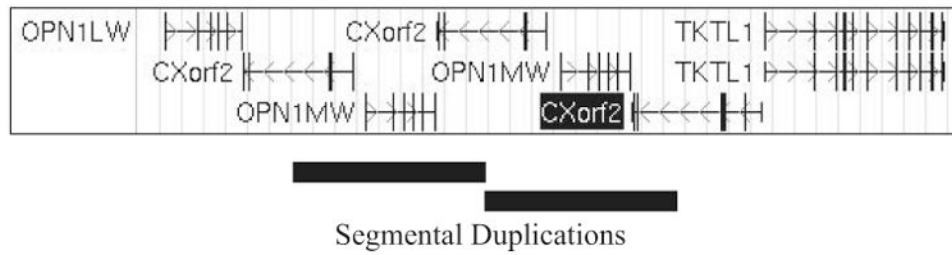


**Figure 1.**

Schematic representation of the arrangement of opsin gene array and *TEX28* genes at the chromosome Xq28 locus (source, UCSC Genome Browser [<http://genome.ucsc.edu/>]). *OPN1LW*, red cone pigment gene; *OPN1MW*, green cone pigment gene; *TKTL1*, transketolase-related gene. *Vertical bars*: exons. *Horizontal bars*: introns. *Arrowheads*: direction of transcription. *Black blocks*: repetitive segments of DNA.

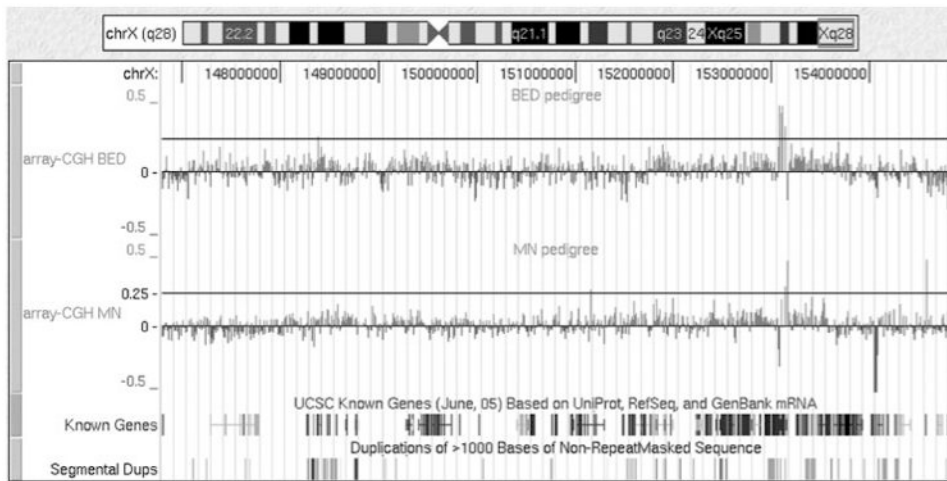


**Figure 2.**

Fine-tiling array-CGH analysis screening for copy number variations on the MYP1 (Xq28) locus in the BED and Minnesota pedigrees. Both pedigrees showed predicted duplications of the opsin gene array (approximately at 153 megabases), whereas the Minnesota pedigree showed an additional intergenic deletion and an intergenic duplication (approximately at 154 megabases). Array-CGH y-axis represents  $\log_2$  ratio (calculated by subtracting the log value of the reference sample intensity from the log of the test sample intensity);  $y = 0.25$  is considered a variation. Average probe spacing was 340 bp. Data were uploaded as custom tracks on to the University of California at Santa Cruz genome browser (<http://genome.ucsc.edu/>) for visualization and comparison.

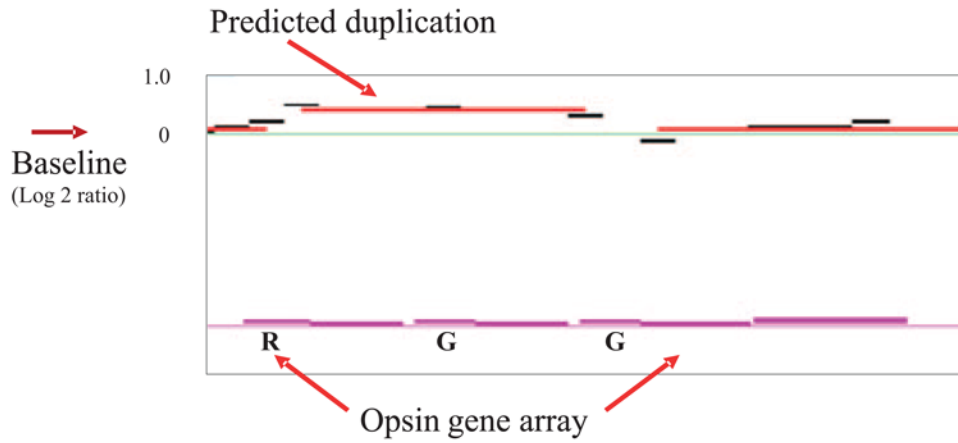


**Figure 3.**

Close-up view of the duplication detected in the region of the opsin gene array. Reference (unaffected male from within the pedigree) and test (affected male from within the pedigree) DNA samples were differentially labeled with fluorescent tags (Cy5 and Cy3, respectively), and hybridized to genomic arrays. The fluorescence ratio (Cy3/Cy5) was determined to reveal copy number differences. The  $y$ -axis represents the  $\log_2$  ratio of Cy3 and Cy5 intensities, and the *horizontal red lines* represent the duplications predicted by a sequence array algorithm.

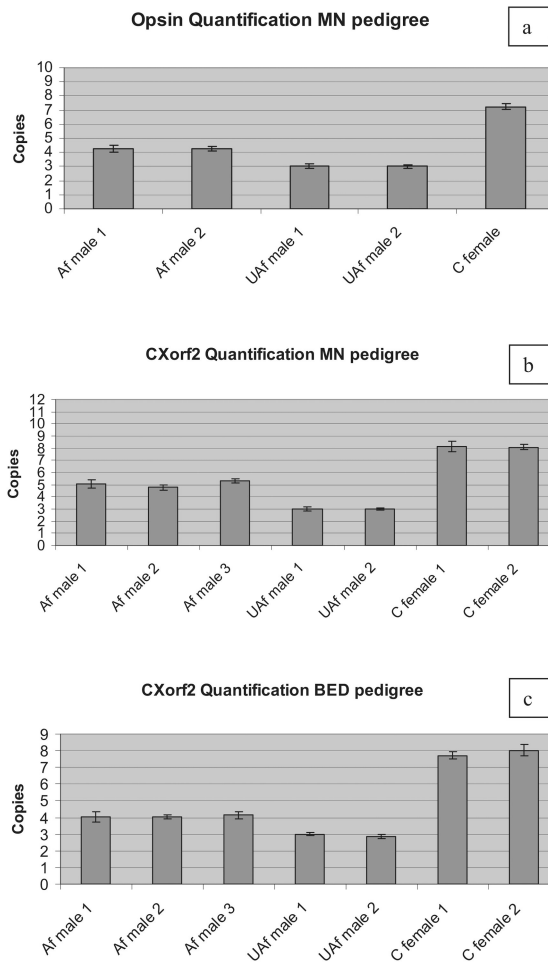


**Figure 4.**

Quantification of opsin and TEX28 gene expression by real-time PCR. Opsin expression pattern followed the number of copies previously reported by Young et al.<sup>4</sup> Affected male DNA samples of the BED pedigree had up to four copies and in the Minnesota pedigree had up to five copies of TEX28. The calibrator was assigned a value of three copies based on and relative to the findings of the number of known copies of opsin gene array. Af, affected; UAf, unaffected; C, carrier. Error bars represent  $\pm$  SEM.

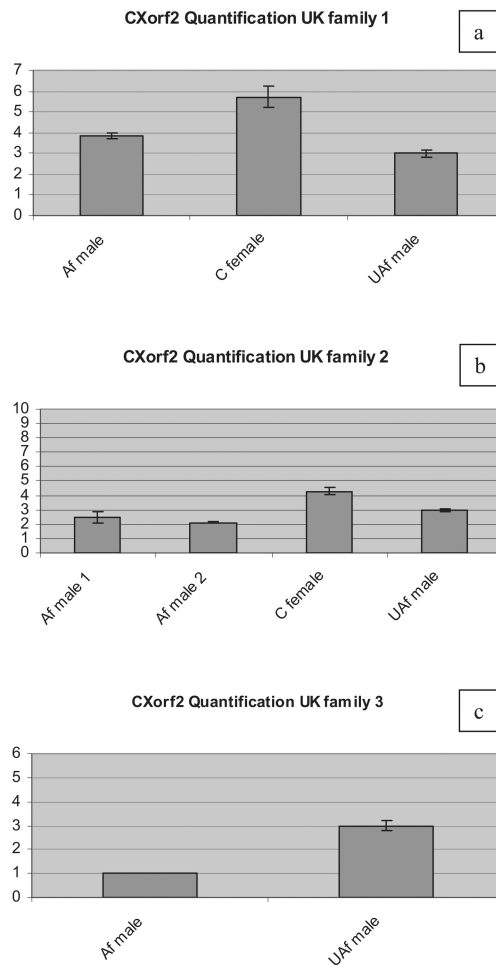


**Figure 5.** Quantification of TEX28 gene expression by real-time polymerase chain reaction in DNA samples of United Kingdom pedigrees. The calibrator was assigned a value of three copies. Family 1 revealed more TEX28 copy numbers in DNA samples of affected males, and Family 3 revealed fewer copy numbers. Af, affected; UAf, unaffected; C, carrier. Error bars represent  $\pm$  SEM.

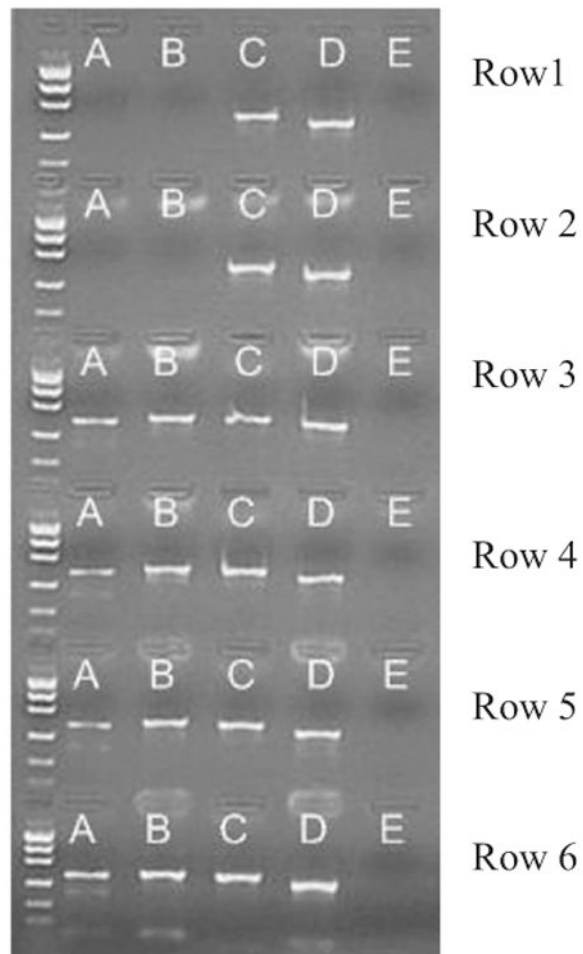


**Figure 6.**

Validation of the 28-kb deletion exclusive to the Minnesota family using PCR. Primer pairs within and flanking the deletion (predicted location, 154046000–154074000 bp) were used. *Rows 1, 2*: affected males. *Rows 3, 4*: unaffected males. *Rows 5, 6*: external male controls. (A, B) Amplicons within the deletion. (C, D) Amplicons outside the deletion. (E) Negative control.



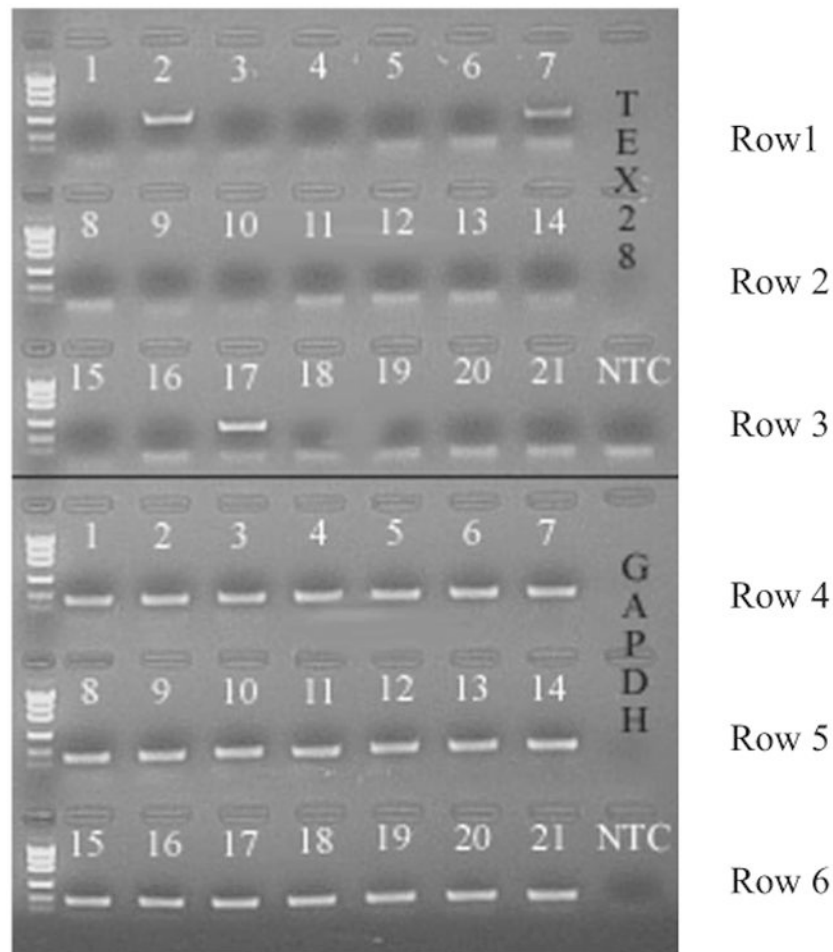


**Figure 7.** Messenger RNA expression of TEX28 in normal tissues determined by reverse transcription polymerase chain reaction. *Rows 1–3:* TEX28 specific primers. *Rows 4–6:* GAPDH-specific primers. 1, adrenal gland; 2, blood; 3, brain; 4, fetal brain; 5, fetal liver; 6, heart; 7, kidney; 8, liver; 9, lung; 10, placenta; 11, prostate; 12, salivary gland; 13, small intestine; 14, skeletal muscle; 15, spinal cord; 16, spleen; 17, testis; 18, thymus; 19, trachea; 20, thyroid gland; 21, uterus; NTC, negative control.

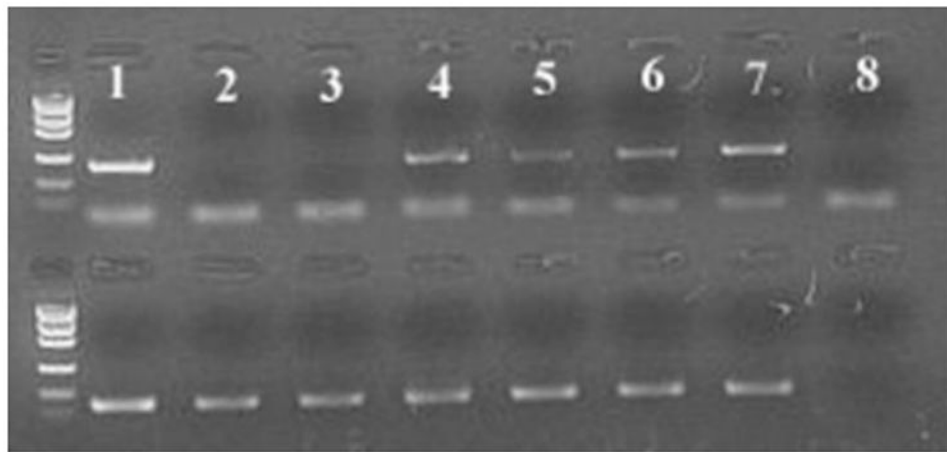


**Figure 8.** Messenger RNA expression of TEX28 in ocular tissues determined by RT-PCR. *Upper row:* TEX28 specific primers. *Lower row:* GAPDH-specific primers. 1, retina; 2, retinal pigment epithelium; 3, choroid; 4, sclera; 5, cornea; 6, optic nerve; 7, trabecular meshwork; 8, negative control.